TOWARDS FAST 3D NANOPARTICLE LOCALIZATION FOR STUDYING MOLECULAR DYNAMICS IN LIVING CELLS

Stefan Sokoll[1,2], Klaus Tönnies[2] and Martin Heine[1]
[1]*Research Group Molecular Physiology, Leibniz Institute for Neurobiology, Magdeburg, Germany*
[2]*Research Group Computer Vision, Otto-von-Guericke University, Magdeburg, Germany*

Keywords: 3D particle localization, Nanometer sub-resolution, Live cell imaging, Confocal fluorescence microscopy.

Abstract: Studying molecular dynamics is crucial for understanding biological processes in living cells. In principle, this is achieved by attaching fluorescent particles to molecules of interest and their detection using fluorescence microscopy. These analysis require fast optical techniques with at least 20Hz frame rate and a resolution below the diffraction limit in all three spatial dimensions. Current approaches basically rely on determining the correlation between features of the particle's 2D point spread function (PSF) and the focal distance to the center of the particle. However, they are still unsuitable for the application to live cell imaging where the refractive index mismatch is present. This mismatch leads to non-stationary optical properties of the particles on which the algorithms rely, necessitating a calibration procedure prior to every experiment. However, this is almost unfeasible to particles attached to living cells.
We established a spinning disk confocal setup and employ Quantum dots (QD) as fluorescence particles. Corresponding models of the axial PSF features that define the distance to the center of the particle are developed and analyzed in the presence of the refractive index mismatch. We present this analysis as the base for the future development of a 3D localization technique applicable to living cells.

1 INTRODUCTION

Neurons are polarized cells that communicate via synapses with each other. Each synapse consists of a pre- and post-synaptic side, with the flow of information going from the former to the latter. Basically, on the arrival of a signaling action potential at a chemical synapse, the interplay of different molecules at the pre-synapse may lead to a release of neurotransmitters into the synaptic cleft (see Figure 1). After absorbance by receptors at the post-synaptic side, neurotransmitters may be again converted into a signaling potential.

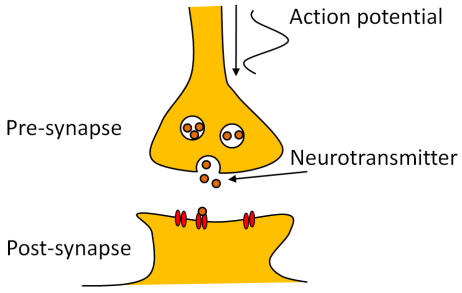

Figure 1: Signal transmission at a chemical synapse.

The probability of successful signal transmission between the pre- and post-synaptic side is liable to strong variation, which is called synaptic plasticity. It is believed to be fundamental for learning and memory. Many different molecules participate in synaptic transmission, e.g. adhesion molecules, receptors, and voltage-gated ion channels. In order to be successful, their arrangement, number, and density seems to be very important. In particular, molecular dynamics at the active zone of the pre-synapse, which describes the area of possible neurotransmitter release, are of special interest.

A well established technique for studying molecular dynamics in living cells is the attachment of fluorescent particles at molecules of interest and their detection using fluorescence microscopy. This procedure involves the acquisition of time-series images, either solely two-dimensional or taken at different focal positions combined to three-dimensional stacks. The trajectories of single particles are then computed from the particular position in each acquisition (see Figure 2).

Studying molecular dynamics requires the optical techniques to perform with at least 20Hz frame rate

Sokoll S., Tönnies K. and Heine M..
TOWARDS FAST 3D NANOPARTICLE LOCALIZATION FOR STUDYING MOLECULAR DYNAMICS IN LIVING CELLS.
DOI: 10.5220/0003166502100215
In *Proceedings of the International Conference on Bioinformatics Models, Methods and Algorithms* (BIOINFORMATICS-2011), pages 210-215
ISBN: 978-989-8425-36-2

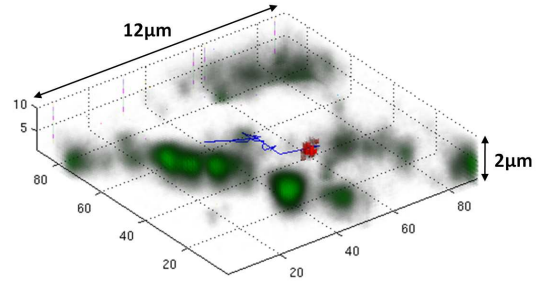

Figure 2: Microscopic 3D image of a QD (in red) and its preceding trajectory (in blue), together with synapses (in green), allowing colocalization analysis.

and a resolution at the molecular level in all three spatial dimensions. For biological applications, 20Hz frame rate are necessary to distinguish different types of molecular diffusion by their diffusion coefficients. High spatial resolution in all three dimensions is especially required as the active zone is usually not bigger than 100-500nm in size and does not necessarily reside in plane with the focal plane of the microscope. To date, various approaches have been developed, but these techniques are only suitable in the absence of the refractive index mismatch, which is the deviation of the refractive indices between the objective's immersion medium and the observed biological medium. As this mismatch is unavoidable in live cell imaging, the optical properties of the particles on which the algorithms rely, cannot be expected to be stationary along the optical axis (Hell et al., 1993). Thus, a calibration has to be performed prior to every experiment, which is almost unfeasible to particles attached to living cells and remains a major challenge.

In this paper, we present a model for the optical properties of Quantum dot (QD) nanoparticles, imaged with a spinning disk confocal setup, and analyze it in the presence of the refractive index mismatch. We first highlight recent developments in the field of single nanoparticle localization followed by the presentation of our axial model. Furthermore, we analyze the model qualitatively and finally conclude that the influence of the refractive index mismatch has to be considered.

2 RELATED WORK

In confocal fluorescence microscopy, the spatial resolution is limited to 200-300nm in the lateral and about 500-700nm in the axial direction by the diffraction of light (Huang et al., 2009). Thus, the image of every sharp spot on the object appears with a blurred intensity profile in the image plane of the microscope. This is referred to as the point spread function (PSF) of the microscope and defines the minimal distance of two light sources such that they can still be resolved in the image.

Localization microscopy is a reasonable technique to overcome this limitation ((Schmidt et al., 1996), (Kubitscheck et al., 2000), (Cheezum et al., 2001)). For two-dimensional images, this technique basically comprises the fitting of a Gaussian function to the PSF of a particle (see Figure 3). Thus, at least the center

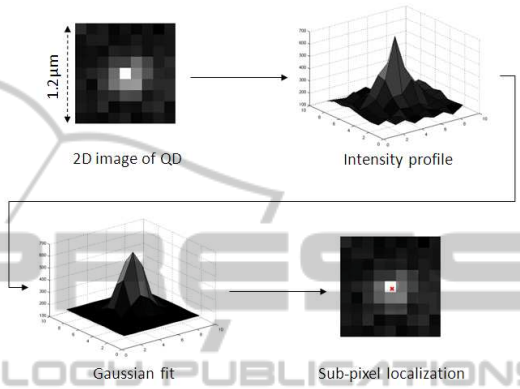

Figure 3: Principle of localization microscopy, leading to sub-pixel localization accuracy.

of a particle can be determined with higher accuracy than the resolution, leading to an accuracy δx approximated by

$$\delta x = \frac{s}{\sqrt{N}}, \tag{1}$$

where s is the standard deviation of the PSF and N the number of collected photons (Thompson et al., 2002).

By analyzing image stacks, this technique is in principle extendable to 3D. The axial center of the particle is defined by the minimum standard deviation of the Gaussian fits in all slices ((van Oijen et al., 1998), (Schütz et al., 2000), (Ragan et al., 2006)). However, such approaches show only a poor time resolution due to the necessity to acquire multiple images for one stack, leading to deformations of the PSF induced by particle movement (see Figure 4). Re-

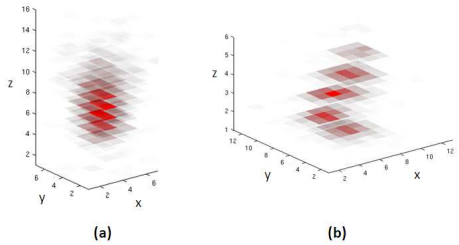

Figure 4: (a) shows the symmetric 3D PSF of an immobile particle. Due to particle movement, the PSF shown in (b) is deformed.

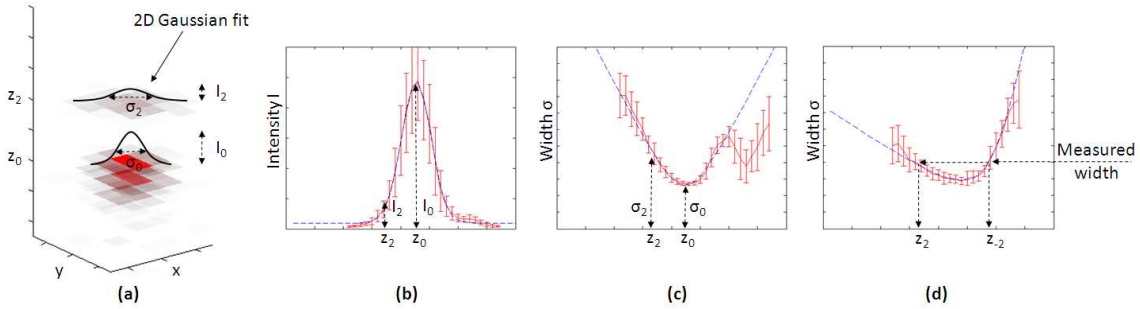

Figure 5: Axial dependency of 2D PSF features. (a) Illustrates the computation of the 2D PSF features of a 3D particle. The resulting approximations to the Gaussian intensity and the parabolic width curve are presented in (b) and (c), respectively. The measurements, together with the standard deviations, are shown in red and the approximations to the measurements in blue. The parabola becomes asymmetric (d), if the refractive indexes differ. Knowing the particular curve, allows the computation of the ambiguous distance to the center of the particle from a single measurement.

cently developed techniques allow the computation of the axial position from one image slice by defocusing the image ((Speidel et al., 2003), (Wu et al., 2005)) or introducing an astigmatism into the light path ((Kao and Verkman, 1994), (Holtzer et al., 2007)). The basic principle amounts to determine the correlation between features of the 2D PSF and the focal distance to the center of the particle. However, due to the refractive index mismatch this correlation varies with the depth of the particle within the biological medium and needs to be adjusted for each experiment. This makes current algorithms unsuitable for live cell imaging as particles attached to molecules of living cells cannot be immobilized for calibration.

3 AXIAL MODEL

The presented techniques were mostly carried out on widefield microscopes. We established a spinning disk confocal setup[1], to combine the advantages of improved spatial resolution as well as the ability to image particles that reside deeper within the medium (Inoué, 2006). Decreased signal intensity is the downside of this choice, leading to less accurate localization results (see Equation 1). However, in the future, this tradeoff allows us to apply the technique to thicker brain slices, which are biologically more relevant than primary cultured neurons. As fluorescence particles, we use QDs, which are semiconductor nanoparticles exhibiting excellent photostability and narrow emission spectra (Toomre and Pawley, 2006).

Initially, we analyzed axial scans of QDs that were immobilized below the cover slip such that the refractive index mismatch had no influence. Here we found two features of the PSF that vary with the axial distance of the measurement to the center of the particle. These are the intensity I and the width σ of the fluorescent peaks at each axial position (see Figure 5(a)). They are computed from the height and the full width at half maximum (FWHM) of the Gaussian fits, respectively. As it is depicted in Figures 5(b-c), the axial intensity distribution follows a Gaussian function and the width of the fluorescence peaks matches a parabola.

Considering the refractive index mismatch by immobilizing QDs at different depths below the cover slip, the parabola of the width becomes asymmetric, where the asymmetry correlates with the depth of the particle within the observed medium (see Figure 5(d)). The Gaussian function of the intensity is also slightly skewed for higher particle depths. However, we found the differences to be neglectable and for simplicity of the model, we retain a symmetric intensity distribution at the moment.

Based on our experimental observations, we identified approximations to both curves. The correlation of the intensity is modeled as a Gaussian function given by

$$I(z) = o + h \cdot e^{-\frac{z^2}{2c^2}}, \qquad (2)$$

where o, h and c are the offset, height and standard deviation, respectively. The axial dependency of the PSF's width is described in (Niedrig, 1993) and extending the presented formula to consider the asymmetry introduced by the refractive index mismatch, we get

$$\sigma(z) = \sigma_0 \cdot \sqrt{1 + \left(\frac{z}{d}\right)^2} + m \cdot z, \qquad (3)$$

where d is the focal depth, σ_0 the FWHM in focus and m represents the skewness of the parabola. Solving

[1]In detail, our setup comprises a Nano Focusing Piezo Stage (PRIOR Scientific), an Olympus Microscope (BX51WI), a Yokogawa spinning disk (CSU-X1), and an Andor iXionEM+897 CCD camera.

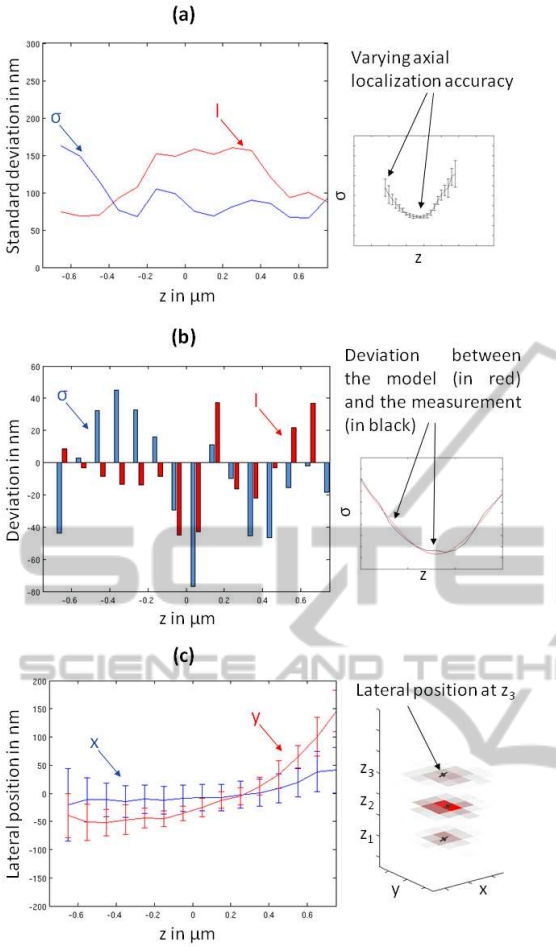

Figure 6: (a-c) Present the axial localization accuracy distribution, the correctness of the axial model and the axial dependency of the lateral position, respectively. All graphs belong to measurements at 5µm depth. (a) and (c) show measurements of individual particles and (b) provides the average result of all particles at this depth. Illustrative examples that explain how the given curves are computed are presented next to each graph.

these equations for z, we can compute the axial position of the particle from only one slice applying either the Gaussian or the parabolic approximation to the intensity or the width, respectively. However, so far the model cannot distinguish if the particle is above or below the focal plane, as it is depicted in Figure 5(d).

4 QUALITATIVE ANALYSIS OF THE MODEL

After introduction of the axial model we now provide further properties that have to be considered for the development of a fast 3D localization algorithm. We present only qualitative results because the final accuracy of the localization depends mainly on the imaging conditions[2].

First, we have analyzed the dependency of the axial localization accuracy on the distance of the image acquisition to the center of the particle (see Figure 6(a)). It becomes apparent that the accuracy distributions of the intensity I and the width σ proceed contrary to each other. The intensity model provides higher accuracy when the particle is off-focus while the width model has best accuracy close to the center position. The shape of these accuracy distributions is typical for all depths, but the localization accuracy worsens with increasing depth. However, the contrary course of the distributions supports the development of a fusion strategy, possibly leading to a constant localization accuracy valid at all axial scan positions.

Next to the axial localization accuracy, the correctness of the approximation to the PSF has to be determined. Figure 6(b) shows the systematic errors of the axial model, computed from the constant deviation of the model to the mean measurements at each axial scan position. It reveals that the measured data twists around the approximation, which is valid for all depths and is consistent with earlier findings from (Schütz et al., 2000). Of course, in principle a more accurate PSF could be computed, however, the correct computation requires the knowledge about optical properties of the setup that are generally not accessible as (Speidel et al., 2003) already pointed out. We consider a more accurate model as a possible future improvement to the accuracy of the localization algorithm. For now we accept that error, which is only in the order of $1/4$ of the localization accuracy and is expected to be reducible via fusion of the models. Furthermore, we found the systematic error to remain constant for all tested depths.

To compute the 3D position of a particle, the dependency of the lateral position on the axial scan position is also required. Figure 6(c) shows that the lateral position varies with different measurements along the axial axis. This hinders the computation of the lateral position independently of the axial position and has to be further investigated. However, at least these curve shapes, presented in Figure 6(c), are generally valid for all particles and depths. Finally, we found that the lateral localization accuracy is best at the center of the particle, which agrees with Equation 1 and slightly improves with increasing depth.

[2]Current data was acquired by imaging of QDs emitting 655nm light with an oil objective of magnification 100x. QDs were illuminated by 488nm light and consecutively scanned for 50ms with z-stacks covering 4µm and a step size of 100nm. 50 z-stacks were acquired of each particle.

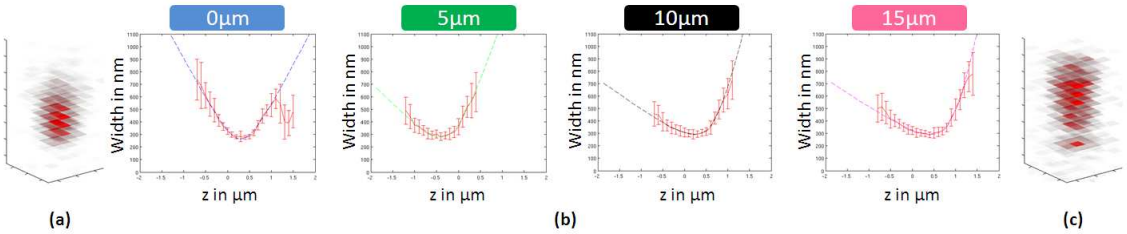

Figure 7: Variation of axial model parameterization for particles at different depths. (b) shows width curve examples for each depth with the measured data in red and the parabolic approximations in a dedicated color. (a) and (c) visualize the PSF for particles at depth 0µm and 15µm, respectively.

5 INFLUENCE OF THE REFRACTIVE INDEX MISMATCH

The presented axial model considers the refractive index mismatch and is valid independently of the particle's depth in the medium. However, the parameters of the model change with varying depths in the medium.

To prove that the consideration of this variation is necessary, we performed calibration measurements at different depths with QDs immobilized in Mowiol and at monolayers of HEK cells[3]. The test set comprises always 40 particles at depths of 0, 5, 10 and 15µm in Mowiol and at 0 and 5µm at HEK cells. Each particle was axially scanned 50 times. Figure 7 depicts example data from width measurements at different depths in Mowiol. The different depths are color coded. It becomes apparent that the curve is symmetric only at zero depth and turns asymmetric for higher depths.

Analysis of the curve parameters revealed that the standard deviation c of the Gaussian and the gradient m of the parabola increase with depth. They uniquely define a certain depth. Figure 8 depicts the different curves when only these classifying parameters are adjusted to the depth and mean values are taken for the remaining ones.

Using wrong parameters for the model will lead to the computation of incorrect axial positions of the particle. For instance, let's assume that a particle was acquired at depth 5µm but is mistakenly expected to be at depth 10µm. Given that, Figure 9 shows the axial position error for each slice in the stack. It is apparent that in this example the error is roughly half as large as the axial localization accuracy presented in Figure 6(a) even though only the classifying parameters are varied. Hence, the error cannot be neglected and this proves that for live cell imaging, where the refractive index mismatch cannot be avoided, calibrating the model parameters is indispensable.

[3]Mowiol is a transparent embedding medium for cell preparations. HEK cells are Human Embryonic Kidney cells, widely used in cell biology research due to their simple handling and fast growth.

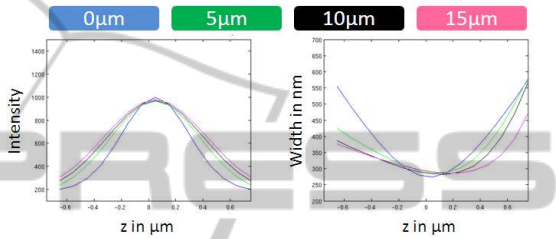

Figure 8: The mean intensity and width curves at different particle depths if only the Gaussian standard deviation c, respectively the gradient m, are adjusted. These findings are valid for Mowiol and HEK cell preparations.

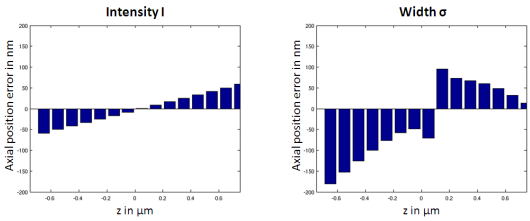

Figure 9: Illustrated are the axial position errors for each model in case one mistakenly expects a particle at depth 10µm instead of its correct position at 5µm.

6 CONCLUSIONS

We presented a model that facilitates the fast 3D localization of nanoparticles in living cells, using a spinning disk confocal setup. We performed qualitative analyzes and described its dependency on the particle's depth in the medium, proving that the refractive index mismatch has to be considered for live cell imaging applications.

We propose two major objectives for future work.

First, we have to develop a localization algorithm that takes the properties of our model into account. Here, major challenges are the ambiguity of the axial model, which we like to address by the introduction of a cylindric lens in the light path as well as a fusion strategy for the intensity and width models to increase the localization accuracy. Second, and far more important, we have to solve the problem that the model parameters cannot be adjusted via calibration. Here, we focus on the estimation of the parameters during each experiment by formulation as an expectation-maximization problem.

ACKNOWLEDGEMENTS

This work is supported by grants from the DFG (HE 3604/2-1).

REFERENCES

Cheezum, M. K., Walker, W. F., and Guilford, W. H. (2001). Quantitative comparison of algorithms for tracking single fluorescent particles. *Biophysical Journal*, 81:2378–2388.

Hell, S., Reiner, G., Cremer, C., and Stelzer, E. H. K. (1993). Aberrations in confocal fluorescence microscopy induced by mismatches in refractive index. *Journal of Microscopy*, 169:341–405.

Holtzer, L., Meckel, T., and Schmidt, T. (2007). Nanometric three-dimensional tracking of individual quantum dots in cells. *Applied Physics Letters*, 90.

Huang, B., Bates, M., and Zhuang, X. (2009). Super-resolution fluorescence microscopy. *Annual Review of Biochemistry*, pages 993–1016.

Inoué, S. (2006). Foundations of confocal scanned imaging in light microscopy. *Handbook of Biological Confocal Microscopy*, pages 1–16.

Kao, H. P. and Verkman, A. S. (1994). Tracking of single fluorescent particles in three dimensions: use of cylindrical optics to encode particle position. *Biophysical Journal*, 67:1291–1300.

Kubitscheck, U., Kückmanna, O., Kuesa, T., and Peters, R. (2000). Imaging and tracking of single gfp molecules in solution. *Biophysical Journal*, 78:2170–2179.

Niedrig, H. (1993). *Lehrbuch der Experimentalphysik*. Walter de Gruyter, Berlin, 9th edition.

Ragan, T., Huang, H., So, P., and Gratton, E. (2006). 3d particle tracking on a two-photon microscope. *Journal of Fluorescence*, 16:325–336.

Schmidt, T., Schütz, G. J., Baumgartner, W., Gruber, H. J., and Schindler, H. (1996). Imaging of single molecule diffusion. *Proceedings of the National Academy of Sciences of the United States of America*, 93:2926–2929.

Schütz, G. J., Pastushenko, V. P., Gruber, H. J., Knaus, H. G., Pragl, B., and Schindler, H. (2000). 3d imaging of individual ion channels in live cells at 40 nm resolution. *Single Molecules*, 1:25–31.

Speidel, M., Jonàš, A., and Florin, E. L. (2003). Three-dimensional tracking of fluorescent nanoparticles with subnanometer precision by use of off-focus imaging. *Optics Letters*, 28:69–71.

Thompson, R. E., Larson, D. R., and Webb, W. W. (2002). Precise nanometer localization analysis for individual fluorescent probes. *Biophysical Journal*, 82:2775–2783.

Toomre, D. and Pawley, J. B. (2006). Disk-scanning confocal microscopy. *Handbook of Biological Confocal Microscopy*, pages 221–237.

van Oijen, A. M., Köhler, J., Schmidt, J., Müller, M., and Brakenhoff, G. J. (1998). 3-dimensional super-resolution by spectrally selective imaging. *Chemical Physics Letters*, 292:183–187.

Wu, M., Roberts, J. W., and Buckley, M. (2005). Three-dimensional fluorescent particle tracking at micron-scale using a single camera. *Experiments in Fluids*, 38:461–465.